Phenomenological theory of the protected nodes and collapse of the Fermi arcs in underdoped cuprate superconductors

Qijin Chen and K. Levin

James Franck Institute and Department of Physics, University of Chicago, Chicago, Illinois 60637, USA
(Received 10 December 2007; revised manuscript received 5 May 2008; published 31 July 2008)

We show how recent angle resolved photoemission measurements addressing the Fermi arcs in the cuprates reveal a very natural phenomenological description of the complex superfluid phase. Importantly, this phenomenology is consistent with a previously presented microscopic theory. By distinguishing the order parameter and the excitation gap, we are able to demonstrate how the collapse of the arcs below T_c into well defined nodes is associated with the *smooth* emergence of superconducting coherence. Comparison of this theory with experiment shows good semiquantitative agreement.

In the past most of the interest in lower T_c cuprate superconductors has focused on the exotic, non-Fermi-liquid normal phase. In a recent paper by Kanigel *et al.*,[1] angle-resolved photoemission spectroscopy (ARPES) experiments on several underdoped samples of $Bi_2Sr_2CaCu_2O_8$ (Bi2212) were used to establish key features of the superconducting phase. In particular, it was reported[1] that (i) the ARPES-measured excitation gap, $\Delta(\mathbf{k}, T)$ is roughly constant in temperature from $T=0$ to above T_c. (ii) Below T_c, $\Delta(\mathbf{k})$ displays the d-wave point nodes which broaden into Fermi arcs above T_c, with the change occurring within the width of the resistive transition at T_c. (iii) It is claimed[2] that the energy scale of the excitation gap is T^*, or the pseudogap[3,4] onset temperature, and that the Fermi arc-length scales with T/T^* above T_c. From (i) it is inferred that (iv) "the energy gap is *not* directly related to the superconducting order parameter."

These latest experiments have underlined the fact that the *superfluid phase* is itself very complex in the presence of a normal-state gap or "pseudogap."[3,4] Some theories[5,6] seem to suggest that the already large pseudogap becomes the order parameter immediately below T_c, which would seem to imply an (unphysical) jump in the order parameter and in the superfluid density, n_s. In our approach we show how these important photoemission observations reveal a more natural description of the superfluid phase. We then review a microscopic model consistent with this phenomenology which has been demonstrated[4] to be compatible with a variety of other experiments and show that it yields good semiquantitative agreement with a large number of different representations of these recent photoemission data.

Our microscopic scheme is based on a BCS–Bose-Einstein condensation (BEC) crossover scenario[4,7] and is distinct from the phase fluctuation scenario.[5,8,9] It has been argued[10] to be appropriate to the cuprates because of their very short coherence length. We emphasize the generic features of our framework. One assumes that there are attractive interactions that lead to pairing which, in turn, gives rise to a gap in the fermionic spectrum. Noncondensed pairs above T_c contribute to this excitation gap, Δ, just as do condensed pairs. Thus, we infer that below T_c, Δ contains two contributions, Δ_{sc} from condensed and Δ_{pg} from noncondensed pairs. Since the pair density is associated with the square of the gap, these contributions add in quadrature to yield

$$\Delta^2 = \Delta_{sc}^2 + \Delta_{pg}^2. \qquad (1)$$

The same equation is consistent with points (i) and (iv) above. Note that the superfluid density $n_s(T)$ is observed to vanish smoothly as T_c is approached from below, which requires that the superconducting order parameter Δ_{sc} turn on continuously as in a second-order phase transition. We then conclude that because the excitation gap $\Delta(\mathbf{k}, T)$ is roughly a constant in T across T_c, there must be another component to the excitation gap below T_c, which compensates for the T dependence in $\Delta_{sc}(T)$. The simplest approach is to think of this term [i.e., $\Delta_{pg}^2(T)$] as a "fluctuation" contribution of the form $\langle \Delta^2 \rangle - \langle \Delta \rangle^2$.

The normal-state analysis of ARPES experiments has already made substantial use[6,11,12] of a broadened BCS form[13] for the fermion self energy

$$\Sigma_{pg}(\mathbf{k}, \omega) = \frac{\Delta_{\mathbf{k},pg}^2}{\omega + \epsilon_{\mathbf{k}} + i\gamma} - i\Sigma_0. \qquad (2)$$

Here the broadening $\gamma \neq 0$ and "incoherent" background contribution Σ_0 reflect the fact that noncondensed pairs do not lead to *true* off-diagonal long-range order. We adopt a tight-binding model for the band dispersion $\epsilon_{\mathbf{k}}$, although the detailed band structure is of no importance in our calculations, which address ARPES data points along the Fermi surface $\epsilon_{\mathbf{k}}=0$. We define $\Delta_{\mathbf{k},pg}=\Delta_{pg}\varphi_{\mathbf{k}}$, and we introduce $\varphi_{\mathbf{k}}=\cos(2\phi)$, to reflect the d-wave $\mathbf{k}$ dependence along the Fermi surface.

In contrast to earlier scenarios[5,6] here we distinguish the superfluid from the normal phases via an additional component of the self-energy arising from the condensate Σ_{sc} so that

$$\Sigma(\mathbf{k}, \omega) = \Sigma_{pg}(\mathbf{k}, \omega) + \Sigma_{sc}(\mathbf{k}, \omega) \qquad (3)$$

$$\Sigma_{sc}(\mathbf{k}, \omega) = \frac{\Delta_{\mathbf{k},sc}^2}{\omega + \epsilon_{\mathbf{k}}}, \qquad (4)$$

with $\Delta_{\mathbf{k},sc}=\Delta_{sc}\varphi_{\mathbf{k}}$. Σ_{sc} is associated with long-lived condensed Cooper pairs and so it is of the same form as Σ_{pg} but without the broadening. With this self-energy in Green's functions, the resulting spectral function, $A(\mathbf{k}, \omega) = -2 \operatorname{Im} G(\mathbf{k}, \omega+i0)$ can be readily determined. One can see

that the spectral function at all $\mathbf{k}$ contains a zero at $\omega = -\epsilon_\mathbf{k}$ below T_c, whereas it has no zero above T_c. This dramatic effect of superconducting coherence will be reflected in the disappearance of Fermi arcs below T_c.

Since Δ_pg represents a contribution from thermal bosonic fluctuations, it should vanish in the ground state and roughly be of the general form

$$\Delta_\mathrm{pg}^2(T) = (T/T_c)^\nu \Delta^2(T_c), \quad T \leq T_c. \tag{5}$$

Using this equation one can determine T_c as the lowest temperature at which $\Delta_\mathrm{sc} = 0$. The exponent ν in general varies between 3 and 3/2, which corresponds to linear and quadratic pair dispersion, respectively. What is important is not the value of ν, but that at T_c the order parameter vanishes, and the term Δ_pg accounts for the entire excitation gap $\Delta(T_c)$.

In the underdoped regime, because $\Delta(T) \approx \Delta(T_c)$, it would appear that the smooth vanishing of the superfluid density n_s at T_c introduces a challenge for theory. In one-gap scenarios[5,6] [which seem to assume $\Delta_\mathrm{sc}(T_c^-) = \Delta(T_c^-)$] one needs to demonstrate explicitly why there is no discontinuity in n_s at T_c. By including two gap parameters below T_c, we arrive at a natural understanding of n_s. Importantly, it is only the condensed pairs which contribute to the Meissner magnetic screening, as expected, so that $n_s \propto \Delta_\mathrm{sc}^2$, which thus vanishes smoothly at T_c. Indeed, this is a natural consequence if one considers superconductivity as Bose condensation of Cooper pairs. The noncondensed pairs discussed above contribute to the destruction of n_s in addition to the usual fermionic terms.[14] These bosonic contributions are clearly required since the number of fermionic excitations ($\propto T/\Delta$) is smaller than the total fermion number for all $T \leq T_c$. The phase fluctuation scenario[8] similarly invokes bosonic excitations to destroy n_s at T_c.

We will show below that, at a semiquantitative level, we can address ARPES data by assuming for all $T < T^*$

$$1 + U\sum_\mathbf{k} \frac{1 - 2f(E_\mathbf{k})}{2E_\mathbf{k}} \varphi_\mathbf{k}^2 = 0, \tag{6}$$

Here $E_\mathbf{k} = \sqrt{\epsilon_\mathbf{k}^2 + \Delta_\mathbf{k}^2}$, with $\Delta_\mathbf{k} = \Delta\varphi_\mathbf{k}$; $U < 0$ is the pairing interaction strength,[14] and $f(x)$ is the Fermi function. The ratio $\Delta(T)/\Delta(0)$ as a function of T/T^* is then given by a nearly universal curve independent of the doping concentration, x. In the underdoped regime, $\Delta(T_c)$ is large so that Eq. (6) is consistent with a very high $T^* \gg T_c$ and a roughly constant gap within the superfluid phase.

We briefly present a T-matrix approach from which Eqs. (1)–(6) were previously derived, noting that more details can be found elsewhere.[4] The BCS-like constraint in Eq. (6) can be interpreted as equivalent to the BEC condition that the noncondensed pairs have zero chemical potential $\mu_\mathrm{pair} = 0$ at and below T_c. This determines the form of the noncondensed pair propagator $t_\mathrm{pg}(Q) = U/[1 + U\chi(Q)]$ such that $t_\mathrm{pg}(0) = \infty$ at $T \leq T_c$, where $\chi(Q) = \Sigma_K G_0(Q-K)G(K)\varphi_{\mathbf{k}-q/2}^2$, is the pair susceptibility. Here G and G_0 are the full and bare Green's functions, respectively. To make direct association with Eq. (6), we drop the γ and Σ_0 term (which are more important above than below T_c) in Eq. (2) and arrive at $\Sigma(\mathbf{k},\omega) \approx \Delta_\mathbf{k}^2/(\omega + \epsilon_\mathbf{k})$ for $T \leq T_c$. This reasonable approximation can

be used to determine the form for G, and establish an equivalence between Eq. (6) and the BEC condition $\mu_\mathrm{pair} = 0$.

To establish the validity of Eqs. (2) and (4), we note that there are two contributions to the full T-matrix $t = t_\mathrm{pg} + t_\mathrm{sc}$ where the condensate contribution $t_\mathrm{sc}(Q) = -\frac{\Delta_\mathrm{sc}^2}{T}\delta(Q)$. Similarly, we have for the fermion self-energy $\Sigma(K) = \Sigma_\mathrm{sc}(K) + \Sigma_\mathrm{pg}(K) = \Sigma_Q t(Q)G_0(Q-K)\varphi_{\mathbf{k}-q/2}^2$, from which Eq. (4) follows at once. A vanishing chemical potential means that $t_\mathrm{pg}(Q)$ diverges at $Q = 0$ when $T \leq T_c$. Thus, in the superfluid phase only, we approximate[13,15] $\Sigma_\mathrm{pg}(K)$ to yield $\Sigma_\mathrm{pg}(K) \approx -G_0(-K)\Delta_{\mathbf{k},\mathrm{pg}}^2$, where $\Delta_\mathrm{pg}^2 \equiv -\Sigma_{Q\neq0} t_\mathrm{pg}(Q)$. We thus may write $\Sigma_\mathrm{pg}(\mathbf{k},\omega) = \Delta_{\mathbf{k},\mathrm{pg}}^2(T)/(\omega + \epsilon_\mathbf{k})$ + small corrections, where we accommodate the corrections[13] with the broadening factor γ and additional term Σ_0. This is necessary in order to address the *concrete* fermion spectral function. In this way, Eq. (2) then follows. Finally, at small four-vector $Q \equiv (\Omega, \mathbf{q})$, we expand the inverse of t_pg, after analytical continuation, to obtain a simple quadratic dispersion[4] for the pairs $\Omega_\mathbf{q} \approx q^2/(2M^*)$, implying $\nu = 3/2$.

To illustrate the simple physics, we do *not* attempt to do detailed curve fitting. We use one set of parameters for all doping x. Thus, in our numerical results we take only Σ_0 and $\gamma(95~\mathrm{K})$ as adjustable to optimize overall fits to the multiple data sets. More concretely, we obtain the universal curve $\Delta(T)/\Delta(0)$ as a function of T/T^* from Eq. (6), say, at optimal doping, and use the experimentally known value of $\Delta(0)$ at given doping concentration x to determine an input T^* and input gap $\Delta(T)$. This value of T^* is to be distinguished from the T^* obtained in ARPES experiments, here called T_ex^*. For our tight binding, quasi-two-dimensional lattice, Eq. (6) yields $2\Delta(0)/T^* \approx 4.3$. In ARPES experiments, T_ex^* is determined as the temperature where γ and Δ are roughly equal so that there is no observable density depletion at the Fermi level. The experimentally deduced ratio from ARPES data[2] is slightly larger than 5 for moderately underdoped samples, and increases with underdoping. A higher ratio of 8 has been observed in *local* STM measurements.[16] The next step theoretically is to use the known T_c to determine $\Delta_\mathrm{pg}(T)$ and $\Delta_\mathrm{sc}(T)$ below T_c, using Eqs. (5) and (1). One can then determine an "experimental" T_ex^* and spectral gap following the ARPES prescription for given parameters γ and Σ_0.

To make this determination, we choose our adjustable parameters Σ_0 and γ via a rough fit to ARPES data near $T_c(\approx 95~\mathrm{K})$ at optimal doping. Since Σ_0 is primarily governed by the particle-hole channel,[11] we take it to be independent of doping and T, and given by $\Sigma_0 = 26$ meV. The broadening parameter γ depends primarily on temperature. Consistent with scattering rate measurements in the literature,[17,18] we take $\gamma = 26$ meV at 95 K, with $\gamma = \gamma(95~\mathrm{K})(T/95~\mathrm{K})$ above T_c and $\gamma = \gamma(T_c)(T/T_c)^3$ below T_c for given doping x, as used earlier.[19] Finally, this yields a ratio $2\Delta(0)/T_\mathrm{ex}^* = 5.6 \sim 5.7$ for the cases presented below, consistent with experiment.[2] Throughout $\phi = 0$ and $\pi/4 = 45°$ denote the antinodal and nodal directions, respectively. In order to compare with ARPES data, we convolve the spectral function with a Gaussian instrumental broadening curve with a standard deviation $\sigma = 3$ meV, given by the ideal ARPES resolution.

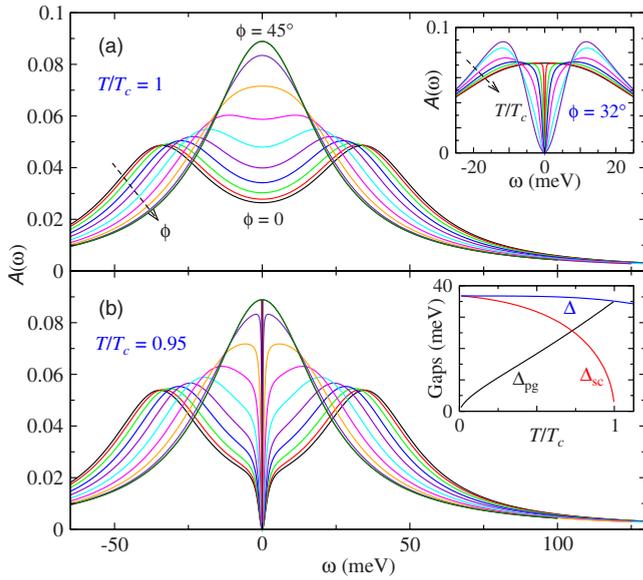In the inset to Fig. 1(b) we plot the various gap param-

FIG. 1. (Color online) Spectral function $A(\omega)$ for $x=0.125$ at (a) $T=T_c$ and (b) $0.95T_c$ at different angles ϕ along the Fermi surface of a cuprate superconductor, where ϕ increases by 4.5° from 0° to 45° along the direction of the arrow. The upper inset shows the temperature dependence of $A(\omega)$ at $\phi=32°$ near the node, with $T/T_c=1$, 0.99, 0.95, 0.9, 0.8, 0.6, and 0.3 in the direction of the arrow. Shown in the lower inset are the gaps vs T below T_c. The effects of phase coherence are more pronounced in the nodal region of the Fermi surface, where the gap is small.

eters Δ_{sc}, Δ, and Δ_{pg} as a function of temperature below T_c and slightly above, for a typical underdoped system. Here for definiteness we have chosen $\nu=3/2$ in Eq. (5). It can be seen that, as T is lowered below T_c, the total excitation gap Δ is essentially a constant while Δ_{sc} increases from 0 at T_c to reach the full gap value at $T=0$. By contrast, Δ_{pg} monotonically decreases to 0.

In Figs. 1(a) and 1(b), we plot the spectral function $A(\omega)$ for $\epsilon_{\mathbf{k}}=0$ (on the Fermi surface) at and slightly below T_c, respectively, and for different angles. To illustrate the physics, here we do not include the ARPES instrumental broadening. Just below T_c, the sharp dip at $\omega=0$ is associated with the onset of a very small condensate, which nevertheless leads to a depletion of the spectral weight at the Fermi level. The coherence associated with the order parameter is better illustrated near the nodal region where a gap, absent at T_c, appears as T decreases, as shown for $\phi=32°$ in the upper inset. A closer inspection of the shape of $A(\omega)$ in Fig. 1(b) suggests that $A(\omega)$ cannot be described by a simple broadened BCS spectral function.

Figure 2 presents a plot of the spectroscopic gap for an underdoped cuprate with $x=0.125$ as a function of angle and for various temperatures below (dashed curves) and above T_c (solid curves). Here the spectral gap is given by half the peak-to-peak distance in the spectral function, and is smaller than the input gap $\Delta(T)$. For $T<T_c$, since the gap is roughly T independent, the various curves tend to coalesce. Above T_c, the extended range of zero gap value around $\phi=45°$ gives rise to the Fermi arcs.[6,12] This is due to the presence of γ. The rapid deviation of the (red dashed) $T=0.99T_c$ curve
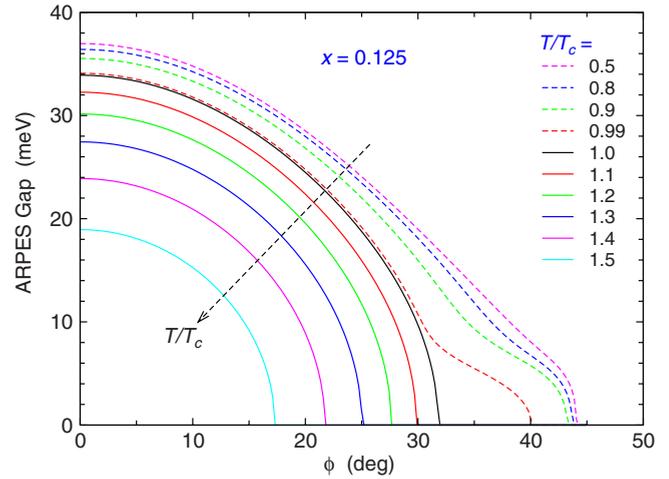

FIG. 2. (Color online) Spectral gap as measured in ARPES as a function of angle ϕ along the Fermi surface of an underdoped cuprate superconductor of doping $x=0.125$, at different T/T_c between 0.5 and 1.5. The spectral function has been broadened with a small ARPES instrumental resolution of 3 meV. A Fermi arc appears as the extended range of zero gap value. The fast departure of the $T=0.99T_c$ curve from the $T=T_c$ curve indicates a collapse of the Fermi arc.

from the (black solid) $T=T_c$ curve indicates a collapse of the Fermi arc, leading to the protected nodes below T_c, reflecting the emergence of superconducting order below T_c. This figure should be compared with Fig. 2 of Ref. 1.

In Fig. 3 we plot the relative loss of spectral weight $L(\phi)=1-I(0)/I(\Delta_\phi)$, defined following Ref. 1, at the antinode $\phi=0$ as a function of T for different doping concentrations, where $I(\omega)\equiv A(\omega)$. This determines T_{ex}^* as where $L(0)$ vanishes. The lower left inset presents plots of $L(\phi)$ as a function of ϕ for various temperatures while the upper right inset illustrates the antinode behavior $L(\phi=0)$ as a function of T/T_{ex}^*. Above T_c the dependence is linear in T, reflecting a linear T dependence in γ. Illustrated in the upper inset is a considerable universality above T_c as a function of T/T_{ex}^*,
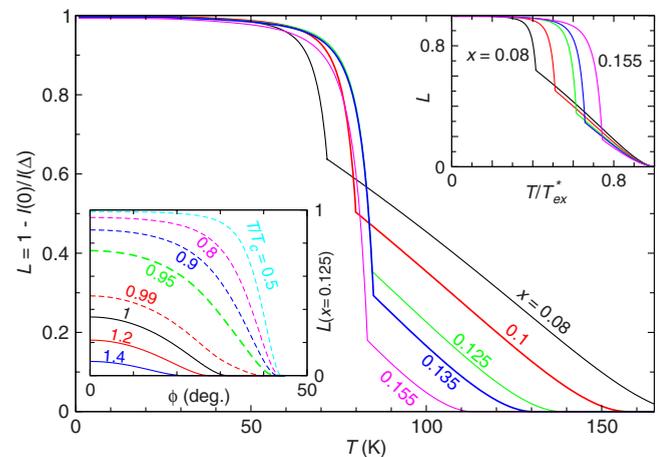

FIG. 3. (Color online) Loss of zero energy spectral weight as a function of temperature at the antinode, for different hole concentrations. Upper right inset shows rescaled T dependence, while lower left inset indicates ϕ dependence for various T.
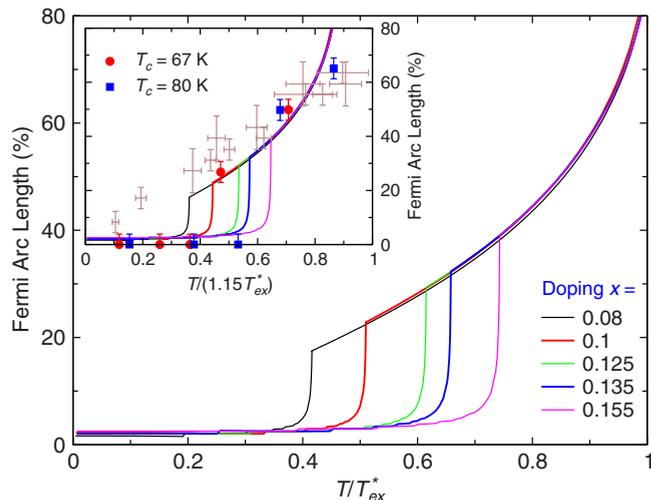
FIG. 4. (Color online) Fermi arc length as a function of T/T_{ex}^* for doping concentrations from optimal to underdoping for a cuprate superconductor. Fermi arc length is typically finite above T_c and drops to zero upon the onset of phase coherence. The normal state portions of the curves is close to universal, in agreement with Ref. 2. The comparison in the inset between the theory with a slightly (15%) enlarged T_{ex}^* and experimental data (symbols) (Ref. 1) shows a good semiquantitative agreement.

which provides a prediction for future ARPES data analysis. As the temperature decreases, the abrupt jump at T_c reflects the onset of phase coherence, as in Fig. 2. Here the $x=0.1$ and $x=0.135$ lines are close to the data for the 67 and 80 K samples in the upper panel of Fig. 4 in Ref. 1.

Finally, Fig. 4 shows the sharp collapse of the Fermi arcs from above to below T_c; we plot the percentage of arc length as a function of T/T_{ex}^* and for different doping concentrations from the optimal to the underdoped regime. The small nonvanishing arc length at low T reflects the finite ARPES resolution. As a consequence of the Fermi arc collapse below T_c, the nodes are "protected." In addition, there is a clear universality seen in the normal state, in good agreement with the central features observed experimentally, shown in Fig. 4 of Refs. 1 and 2. Since the mean-field equation is only a crude approximation above T_c, it is reasonable to allow T_{ex}^* to vary slightly, as we have done here, to compare semiquantitatively with the data. By contrast with Ref. 1, however, our curves are not strictly straight lines, reflecting the nonlinearity of the gap as a function of $\phi - \pi/4$, as also found in Ref. 6; this seems to be consistent with Fig. 4 of Ref. 2.

The microscopic approach[4] considered here is associated with stronger-than-BCS attractive interactions which lead to small pair size. A major consequence of this theory (as well as the equivalent phenomenology which ARPES experiments lead us to infer) is that *pseudogap effects persist below T_c* in the form of noncondensed pair excitations of the condensate. Importantly, this leads to two contributions to the self-energy below T_c [see Eq. (4)]. We find that the collapse of the Fermi arcs is not to be associated with an abrupt disappearance (as assumed elsewhere[6]) of the inverse pair lifetime γ, appearing in Σ_{pg}, but rather it reflects the *gradual* emergence of the condensate, appearing in Σ_{sc}, to which the finite momentum pairs are continuously converted as T decreases.

[1] A. Kanigel, U. Chatterjee, M. Randeria, M. R. Norman, S. Souma, M. Shi, Z. Z. Li, H. Raffy, and J. C. Campuzano, Phys. Rev. Lett. **99**, 157001 (2007).

[2] A. Kanigel *et al.*, Nat. Phys. **2**, 447 (2006).

[3] P. Lee, N. Nagaosa, and X. G. Wen, Rev. Mod. Phys. **78**, 17 (2006).

[4] Q. J. Chen, J. Stajic, S. N. Tan, and K. Levin, Phys. Rep. **412**, 1 (2005).

[5] M. Franz and A. J. Millis, Phys. Rev. B **58**, 14572 (1998).

[6] M. R. Norman, A. Kanigel, M. Randeria, U. Chatterjee, and J. C. Campuzano, Phys. Rev. B **76**, 174501 (2007).

[7] A. J. Leggett, *Modern Trends in the Theory of Condensed Matter* (Springer-Verlag, Berlin, 1980), pp. 13–27.

[8] V. J. Emery and S. A. Kivelson, Nature (London) **374**, 434 (1995).

[9] M. Franz, Z. Tesanovic, and O. Vafek, Phys. Rev. B **66**, 054535 (2002).

[10] A. J. Leggett, Nat. Phys. **2**, 134 (2006).

[11] Q. J. Chen, K. Levin, and I. Kosztin, Phys. Rev. B **63**, 184519 (2001).

[12] A. V. Chubukov, M. R. Norman, A. J. Millis, and E. Abrahams, Phys. Rev. B **76**, 180501(R) (2007).

[13] J. Maly, B. Jankó, and K. Levin, Physica C **321**, 113 (1999).

[14] Q. J. Chen, I. Kosztin, B. Jankó, and K. Levin, Phys. Rev. Lett. **81**, 4708 (1998).

[15] I. Kosztin, Q. J. Chen, B. Jankó, and K. Levin, Phys. Rev. B **58**, R5936 (1998).

[16] K. Gomes, A. Pasupathy, A. Pushp, S. Ono, Y. Ando, and A. Yazdani, Nature (London) **447**, 569 (2007).

[17] A. Hosseini, R. Harris, S. Kamal, P. Dosanjh, J. Preston, R. Liang, W. N. Hardy, and D. A. Bonn, Phys. Rev. B **60**, 1349 (1999).

[18] T. Valla, A. V. Fedorov, P. D. Johnson, B. O. Wells, S. L. Hulbert, Q. Li, G. D. Gu, and N. Koshizuka, Science **285**, 2110 (1999).

[19] See footnote 42 of Ref. 11. We have also checked that below T_c the Fermi arc length is not sensitive to the power law of $\gamma(T)$.